GEOLOGICA BELGICA (1998) 1: 41-48

Conodont deformation in the Naux limestone (Ardennes, France)

Manuel SINTUBIN[1, 2] & Stefan HELSEN[1]

(7 figures)

1. Afdeling Historische Geologie, Katholieke Universiteit Leuven, Redingenstraat 16, 3000 Leuven, Belgie.
2. Postdoctoral Fellow F.W.O. – Vlaanderen (Belgie).

ABSTRACT. To date conodont deformation has rarely been applied in a quantitative strain analysis. Using the exceptional collection of deformed Pa (Platform) elements of *Ozarkodina remscheidensis remscheidensis* (Ziegler, 1960), sampled — without information about their in situ orientation — in the Gedinnian Naux Limestone (Ardenne, France), an attempt is made to use deformed conodont elements as strain markers. Preliminary results show that the strain, suffered by these conodont elements, is relatively low compared to strains measured in the adjacent pelitic and conglomeratic formations. Several deformation patterns can be recognised, indicating shortening or angular shear deformation. However, the applicability of deformed conodont elements as quantitative strain markers remains still to be proven, due mainly to the problem of determining their in situ orientation.

KEYWORDS: Conodont, Strain analysis, Naux (Ardenne).

RESUME. Déformation de conodontes dans le calcaire de Naux (Ardennes, France). Jusqu'aujourdhui la déformation de conodontes est rarement appliquée dans des analyses quantitatives de déformation. En utilisant la collection exceptionnelle d'éléments Pa (Plateforme) d'*Ozarkodina remscheidensis remscheidensis* (Ziegler, 1960), échantillonnée — sans tenir compte de leur orientation en place — dans le calcaire Gedinnien de Naux (Ardenne, France), un essai d'utilisation de ces éléments de conodontes déformés comme marqueur de déformation a été effectué. Les résultats préliminaires montrent que la déformation, enregistrée par les conodontes est relativement faible comparativement aux déformations mesurées dans les formations pélitiques et conglomératiques adjacentes. Différents types de déformation sont reconnus, indiquant des racourcissements ou des cisaillements angulaires. Par contre, la possibilité de l'utilisation d'éléments de conodontes déformés comme marqueur quantitatif de déformation reste à vérifier, surtout à cause du problème lié à la détermination de leur orientation en place.

MOTS-CLES : Conodont, Analyse de déformation, Naux (Ardenne).

SAMENVATTING. Vervorming van conodonten in de Kalksteen van Naux (Ardennen, Frans). Tot de dag van vandaag is de vervorming van conodonten zelden aangewend in een kwantitatieve vervormingsanalyse. Gebruik makend van de uitzonderlijke collectie van vervormde Pa (Platform) elementen van *Ozarkodina remscheidensis remscheidensis* (Ziegler, 1960), bemonsterd — zonder echter rekening te houden met de „in situ" orientation — in de Gedinniaan Kalksteen van Naux (Franse Ardennen), is er een poging verricht deze vervormde conodontelementen aan te wenden als vervormingsindicator. Voorlopige resultaten tonen aan dat de vervorming, opgenomen door deze conodontelementen, relatief laag is vergeleken met de vervormingen gemeten in de boven- en onderliggende pelitische en conglomeratische formaties. Verschillende vervormingspatronen kunnen worden onderscheiden, wijzend op een verkorting of een schuifvervorming. De toepasbaarheid van vervormde conodontelementen als vervormingsindicator blijft echter te bewijzen, vooral omwille van het probleem van de „in situ" orientation van de elementen.

SLEUTELWOORDEN : Conodont, vervormingsanalyse, Naux (Ardennen).

1. Introduction

When conodont deformation is observed, it is usually only mentioned, or even considered as a nuisance for determination and taxonomical classification. Occasionally conodont deformation is described (e.g. Flügel & Ziegler, 1957; Kozur & Mock, 1977; Schönlaub *et al.*, 1980; Raven & Van der Pluijm, 1986; Kovacs & Arkai, 1987; Rejebian *et al.*, 1987; Königshof, 1992). Kovacs & Arkai (1987) associate conodont deformation with medium to high pressure metamorphism, which is reflected in CAI ("Colour Alteration Index") values of 5 or higher (Kovacs & Arkai, 1987; Königshof, 1992). Deformation of conodonts is often of brittle nature and is related to cleavage development. Only contact metamorphism and hydrothermal alteration causes ductile deformation of conodonts (Königshof, 1992). Conodont deformation has, however, rarely been quantified for the purpose of a strain analysis. To our knowledge only Beutner & Charles (1985) used deformed conodont elements as an absolute strain measure in an attempt to determine the volume loss during cleavage development in Ordovician slates (Hamburg Sequence, Pennsylvania).

A new attempt is made here to use deformed conodont elements in a quantitative strain analysis. The exceptional collection of deformed Pa (Platform) elements of *Ozarkodina remscheidensis remscheidensis* (Ziegler, 1960) sampled in the Naux Limestone at its type locality (Naux, France) is considered very suitable for this purpose even though no information is available about the in situ orientation of the individual elements. Questions which have to be answered before conodont elements can be considered as strain markers, are how conodont elements record deformation and if this deformation is representative for the material in which the conodont elements are embedded. To answer these questions such an analysis must include: (1) description of the deformed conodont elements; (2) classification of the deformed conodont elements to distinguish deformation patterns; (3) quantitative appraisal of the deformation; (4) in situ orientation study of the conodont elements, enabling a determination of the relationship between conodont element orientation and the structural framework (bedding, cleavage, lineation); (5) a rheological study of the conodont elements, to determine their behaviour in a deforming matrix; (6) correlation with other means of quantitative strain determination, to determine the significance of the conodont deformation. At the current stage of the research only results can be presented on the distinction of deformation patterns, the quantitative appraisal of the deformation, and the correlation with other strain markers. On the in situ orientation of the conodont elements only some assumptions will be made, based on the structural framework obtained from other strain measures.

2. Geological setting

Conodonts were sampled in an outcrop of the Naux Limestone in the Semoy Valley at the type locality Naux (Ardennes, France) (Borremans & Bultynck, 1986) (Fig. 1). The Naux Limestone is part of the Fépin Formation (Meilliez, 1984), which forms the basal sequence of the Gedinnian around the Rocroi Basement (Fig. 1). The Naux Limestone has a limited and lenticular occurrence on the southern limb of the Rocroi Basement and is interpreted as a reef-like structure, associated with normal growth fault activity along the southern border of the basement, active during Devonian basin development. The growth fault is inverted in the Variscan orogeny, forming the Bogny Fault (Meilliez *et al.*, 1991) (Fig. 1). The conodont fauna in the Naux Limestone indicates a Latest Pridolian to Earliest Lochkovian age (Borremans & Bultynck, 1986), which implies that the basal formations of the Gedinnian around the Rocroi Basement may very well be of Late Silurian age. A Colour Alteration Index (CAI) of 5 to 5.5 and various recrystallisation features on the conodont elements (Helsen & Königshof, 1994; Helsen, 1994) shows epizonal metamorphic conditions.

The Naux Limestone is a massive, heterogeneous, crinoidal limestone with schistose intercalations. It is mainly composed of a micritic to sparitic calcite matrix with large, irregular, quartz grains and fine-grained quartz aggregates. Macrofossils are crinoids and bryozoans. The only clear deformation features observed in the limestone are the extensive twinning of calcite, the undulose extinction of quartz and irregular stylolithic seams. Moreover, the crinoid sections are slightly elliptical. It is, however, not obvious that this is the reflection of a deformation, and not just due to oblique sections of the crinoid columns. In the more heterogeneous limestone with higher concentrations of quartz and phyllosilicates a rough cleavage fabric developed at an angle of 40° (south-dipping) to the subhorizontal bedding. The cleavage has an anastomosing character around the lens-shaped quartz grains and quartz aggregates. The fabric shows an anisotropy in the cleavage plane. Extensional components, such as mica beards around quartz grains and pressure shadows around crinoid sections, are indeed only observed in submeridional sections perpendicular to the cleavage fabric. The cleavage development is much more pronounced in the adjacent, more pelitic, material.

3. Conodont deformation

The strain analysis is performed exclusively on Pa (Platform) elements of *Ozarkodina remscheidensis remscheidensis* (Ziegler, 1960), because of their abundance in the Naux Limestone. This subspecies belongs to the *woschmidti* Conodont Zone. The following results are based on the analysis of 60 specimens. Examples of these deformed conodont elements can be found on Plate 4 in Helsen (1994).

The strain analysis is performed on micrographs taken on a Scanning Electron Microscope (SEM) of the conodont elements in top view. This orientation is considered the most suitable, because the deformation commonly occurred perpendicular to this direction.

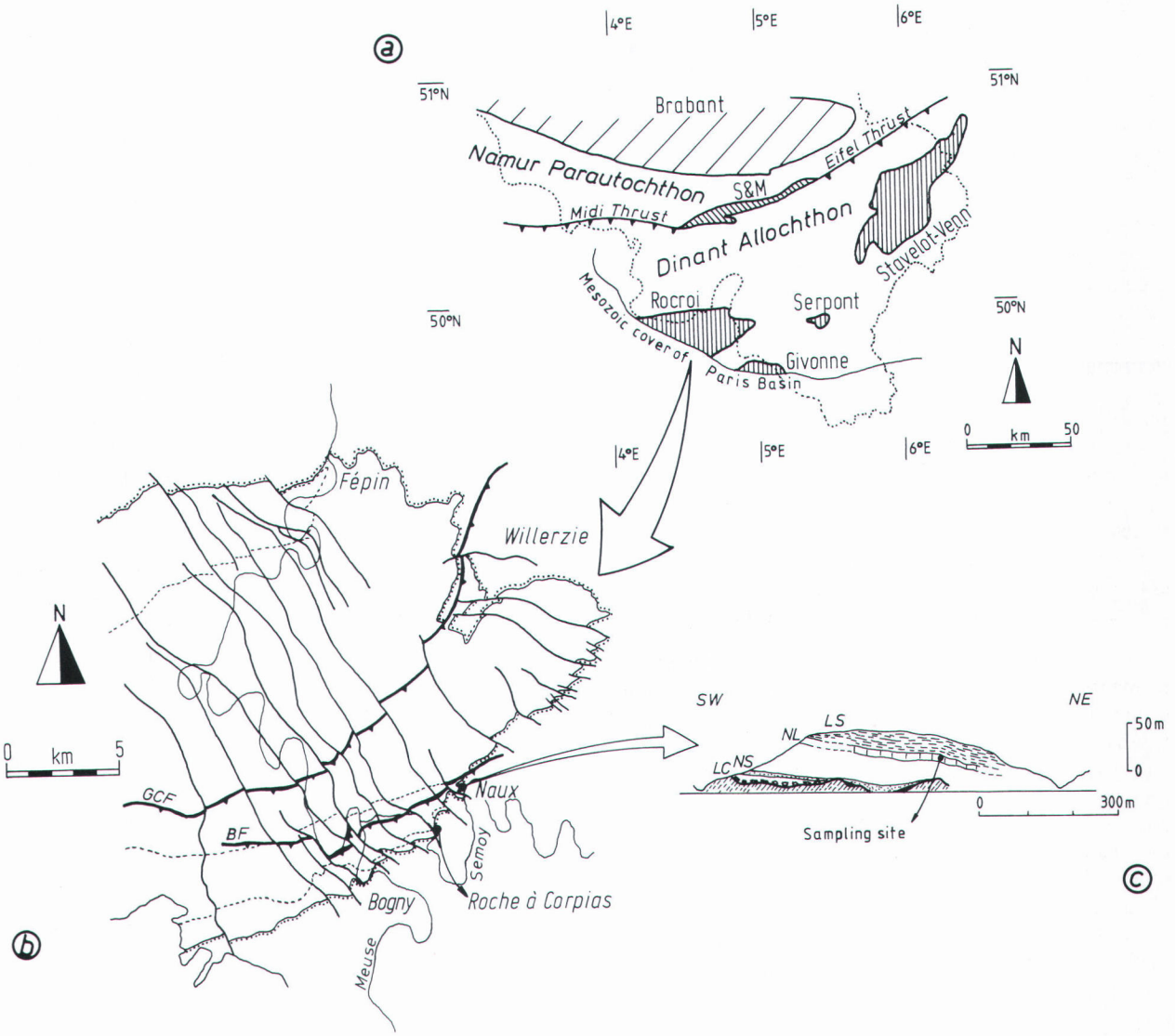

Figure 1. (a) Schematic map of the major structural domains of the Variscan fold-and-thrust belt in Belgium, with indication of the different Lower Palaeozoic basement massifs (Brabant, S & M = Sambre-et-Meuse, Rocroi, Serpont, Stavelot-Venn, Givonne). The Variscan front complex, separating the Dinant Allochthon from the Namur Parautochthon, consists of the Midi and Eifel Thrusts and the Sambre-et-Meuse basement massif; (b) Schematic map of the eastern part of the Rocroi Massif (after Beugnies, 1963) (GCF = Grande Commune Fault; BF = Bogny Fault) (Hugon, 1983); (c) Sampling site at Naux (Ardennes, France) (LS = Lévrezy Slates; NL = Naux Limestone; NS = Naux Sandstone; LC = Linchamps Conglomerate) (after Borremans & Bultynck, 1986).

Pa elements of *Ozarkodina remscheidensis remscheidensis* consist of a nearly straight blade with denticles of unequal height and a basal cavity positioned in the centre of the blade (Fig. 2). Structural elements to be considered in the strain analysis are the curvature of the blade, the angular relationship between blade and denticles and the angular relationship between blade axis and basal cavity axis. In undeformed *Ozarkodina* Pa elements these two axes form an angle of 90° with each other.

An estimation is made of the overall extension $e = (l-l_0)/l_0$. The original length of the conodont element (l_0) is measured along the blade, while the current length (l) is measured between both extremities of the conodont element (Fig. 3). The specimens used are, however, incomplete. We therefore assume that the extension, measured on the incomplete specimens, is representative for the whole conodont element.

Different deformation patterns can be distinguished (Fig. 4):

a) **Kinking**: Kinking of the blade occurs in between denticles. The kink angle ranges from 25° to 90°. The location of the kinks is often determined by the position of the basal cavity. The overall extension ranges from -0.25 to -0.03, with a mean extension of -0.08.

b) **Buckling**: The distinction between buckled and kinked conodont elements is arbitrary. Buckling is independent

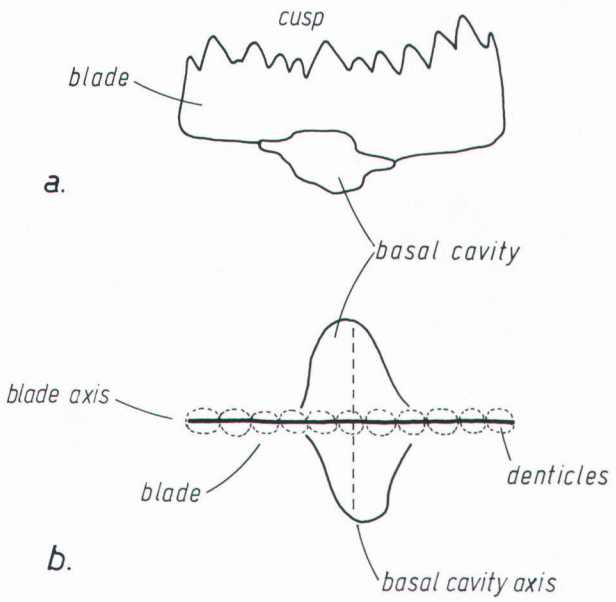

Figure 2. Pa (Platform) element of *Ozarkodina remscheidensis remscheidensis*: (a) side view (after Ziegler, 1960); (b) idealised top view. The size of an element is approximately 500 mm.

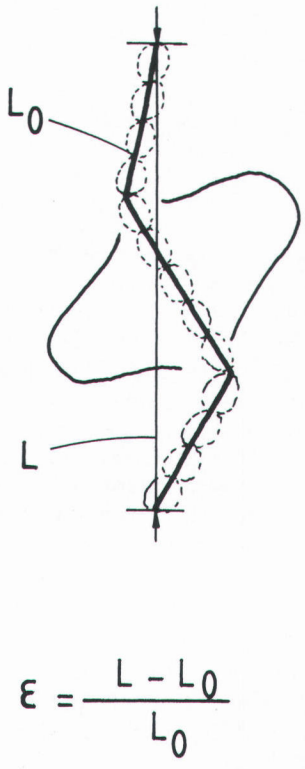

Figure 3. Estimation of the extension $e = (l - l_0)/l_0$ on an *Ozarkodina* Pa element (top view).

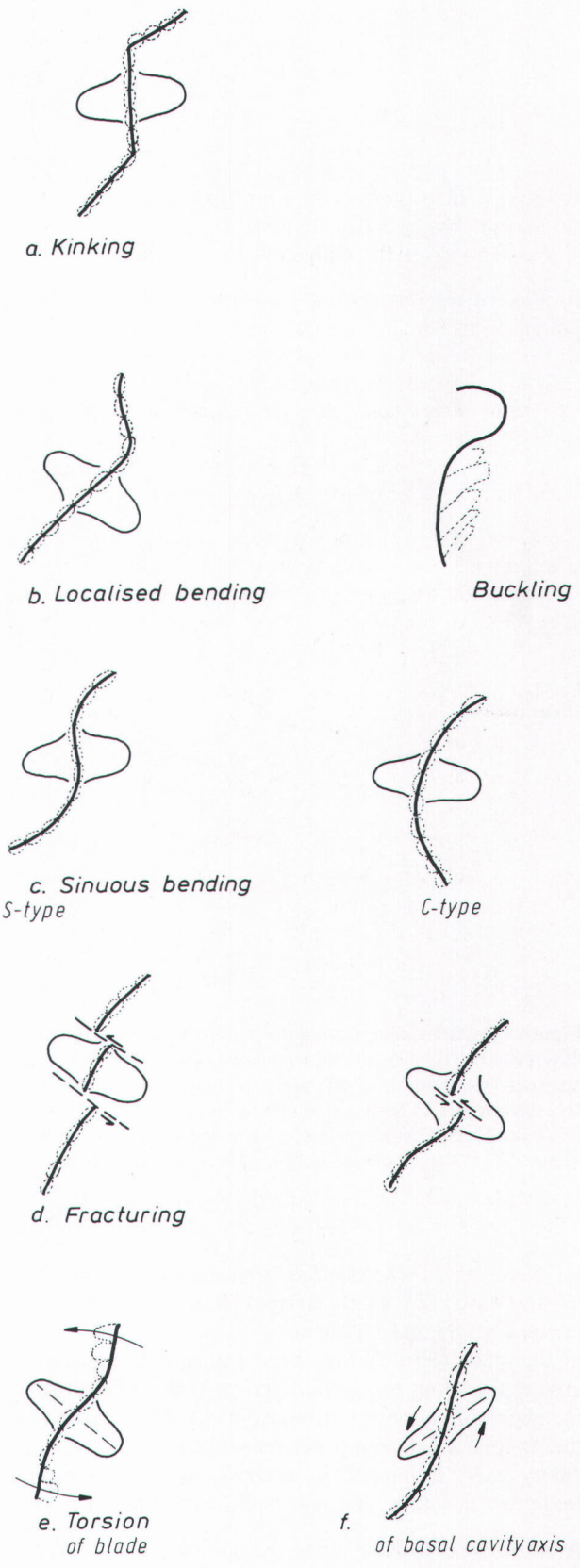

Figure 4. Different deformation patterns of *Ozarkodina* Pa elements.

of the denticle position on the blade, as well as independent of the basal cavity position. The angle ranges from 45° to 90°. Buckling not only occurs perpendicular to the length axis of the conodont element, but also parallel to this axis. The overall extension ranges from – 0.45 to – 0.08, with a mean extension of – 0.22.

c) **Sinuous bending**: Most conodont elements are slightly deformed by a sinuous bending of the blade. Two types of bending occur: S-type and C-type. This bending is often associated with torsion of the blade or fracturing. The overall extension is minimal and ranges from – 0.14 to – 0.01, with a mean extension of – 0.06.

d) **Fracturing**: Conodont elements may also be fractured. These fractures commonly occur perpendicular to the blade in between denticles. The emplacement of fractures is either determined by the basal cavity position. Otherwise fracturing occurs above the basal cavity. In the latter case, differential torsion of the blade took place. The extension is minimal. These fractures indicate a shear deformation rather than an extension.

Another feature is the occurrence of mica crystals in the fractures. These crystals may have grown during cleavage development, and can therefore be of help in a first attempt to determine the in situ orientation of the conodont elements (see Fig. 7).

e) **Torsion of the blade**: In combination with the previously described deformation patterns a torsion of the blade can occur around an axis parallel to the length of the conodont element. This torsion can be in the same or opposite directions on either side of the basal cavity. Rarely, torsion occurs above the basal cavity.

f) **Torsion of the basal cavity axis**: The angular relationship between blade axis and basal cavity axis sometimes shows a deviation from the expected 90°. This indicates a shear deformation. The shear angle γ ranges from 10° to 40°.

Although deformation can be independent of the basal cavity position (Fig. 5a), in the majority of the deformed conodont elements the basal cavity seems to have played a role in localising the deformation. On the one hand, the deformation can be localised along the sides of the basal cavity (Fig. 5b). On the other hand, the deformation of the blade can be situated directly above the basal cavity (Fig. 5c), in which case the deformation dies out towards the basal cavity.

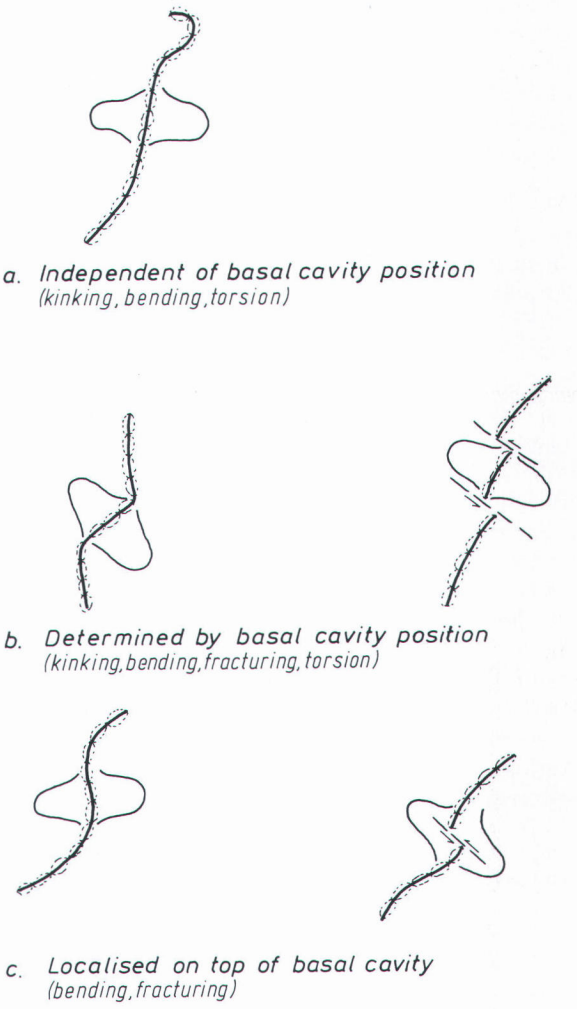

Figure 5. Relationship between deformation of *Ozarkodina* Pa elements (top view) and basal cavity position.

4. Discussion

The different deformation patterns indicate shortening, angular shear strain and fracturing. No extensional patterns, such as boudinaged conodont elements (cf. Beutner & Charles, 1985), are observed. Probably such broken conodont elements are lost during conodont extraction and are only observable in situ.

The degree of strain obtained from the conodont elements is rather low. The mean extension is – 0.1. This limited strain agrees with the nearly undeformed aspect of the crinoid sections. The Naux limestone seems to have undergone limited internal deformation, contrary to the adjacent, more pelitic formations, in which a pronounced slaty cleavage developed. The mean extension perpendicular to the cleavage plane, calculated from the phyllosilicate preferred orientation (see Sintubin, 1994), ranges from – 0.59 (mica) to – 0.61 (chlorite) (Fig. 6).

The conodont deformation is clearly of tectonic nature. It is indeed believed that compaction and subsequent passive bending around quartz grains are not responsible for the conodont deformation. Quartz grains observed on the SEM-micrographs are actually too small to cause this deformation. Moreover, if passive bending of conodont elements around hard grains is the deforming mechanism, deformed conodont elements should be a more common feature in both metamorphic and diagenetic rocks.

At this point no further steps in the strain analysis can be made unless the in situ orientation of the conodont elements is determined. An orientation study of conodont

elements in situ is, however, excessively tedious. Such a study needs the systematic dissolution of bedding-parallel sections of the limestone with regular checks whether conodont elements are visible. Other options for such a study are based on the density contrast between the conodont apatite and the matrix minerals, for instance in X-ray contact microradiography (Norby & Avcin, 1987).

An attempt to explain the observed deformation patterns is achieved by a reversed approach, starting from the kinematic framework, determined by a strain analysis in the adjacent formations. In the Linchamps Conglomerate at "Roche à Corpias" (2 km to the SW — Fig. 1b) an Rf/f-analysis (Ramsay & Huber, 1983) of the conglomerate pebbles has been carried out (Meilliez, 1984). On the Lévrezy Slates, just above the Naux Limestone (Fig. 1c), an analysis of the preferred orientation of mica and chlorite is performed (Fig. 6). Both analyses show a predominantly flattening regime, generating a cleavage at an angle of 40° (dipping to the South) with the subhorizontal bedding, with a significant, submeridional, stretching in the flattening plane. The strain obtained in the slates is higher than that obtained in the conglomerates, indicating a lithology-dependent partitioning of strain. Moreover, in the more schistose limestone mica beards along quartz grains and pressure shadows around crinoid sections, both observed only in submeridional sections perpendicular to the cleavage, also indicate the submeridional stretching in the cleavage plane.

Now consider the settling of conodont elements. Although experiments on the hydrodynamic behaviour of various conodont elements, i.e. settling velocities and sorting, were carried out by Broadhead & Driesse (1990) and Mc Goff (1991), accurate information on the settling position of *Ozarkodina* Pa elements is scarce. However, studies on Carboniferous polygnathacean conodont apparatuses, based on bedding plane assemblages (Aldridge *et al.*, 1987) and the finding of an *Ozarkodina* bedding plane assemblage (Mashkova, 1972), indicate a flat-lying blade with upright basal cavity as the most stable settling position.

Based on this preferential settling position and the kinematic framework, an attempt can now be made to explain the observed deformation features of the conodont elements (Fig. 7). Considering the angular relationship between bedding and cleavage (40°) an overall bedding-parallel shear strain can be assumed. In such kinematic framework the bedding plane (= shear plane) is a "plane of no finite strain". The near-parallelism of the conodont blades with this "plane of no finite strain" may therefore very well be the reason for the relative low degree of conodont deformation. Kinking and buckling are the obvious effects in this orientation because the blade is oriented in the compressional sectors of the finite strain ellipsoid. In this orientation the planes, in which mica has grown, are parallel to the plane of maximum flattening, and thus parallel to the cleavage plane. To explain the torsion of the basal cavity axis, finally, a simple shear component, which eventually may be responsible for the stretching in the cleavage plane, is assumed.

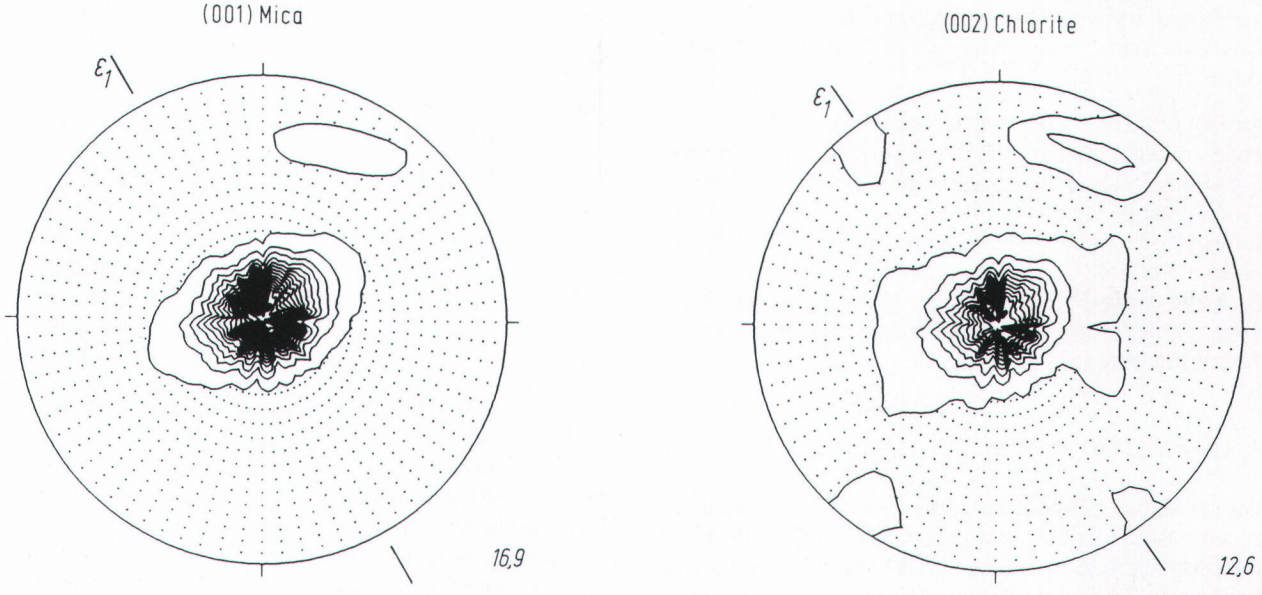

Figure 6. Mica and chlorite textures in the Lévrezy Slates (pole figure centred around cleavage pole; equal-area lower-hemisphere projection; contours = 1 mrd (= "multiple of random distribution"); dotted area < 1 mrd). The orthorhombic pole figure pattern is indicative for an apparent flattening regime with significant stretching in the flattening plane (Sintubin, 1994). The principal extension direction ε_1 coincides with the mesoscopic stretching lineation direction. The March (1932) strain for mica equals [0.71 0.51 - 0.61] and for chlorite [0.61 0.44 -0.57] (see Sintubin (1994) for an extensive discussion on the calculation of March Strains).

5. Preliminary conclusions

The observed deformation patterns of the Pa elements of *Ozarkodina remscheidensis remscheidensis* in the Naux Limestone indicate shortening and shear deformation but no stretching. The estimated strain values are low, probably due to the low internal deformation of the limestone, as also indicated by the nearly undeformed crinoid sections. An in situ orientation study of the conodont elements is the principal obstacle for their use as strain markers. All potential methods to reveal the in situ orientation would be very time consuming, and we doubt their practicality as a standard procedure. All the same, it would be interesting to verify whether deformed conodont elements could be used for a quantitative strain analysis in special cases, where all other methods fail.

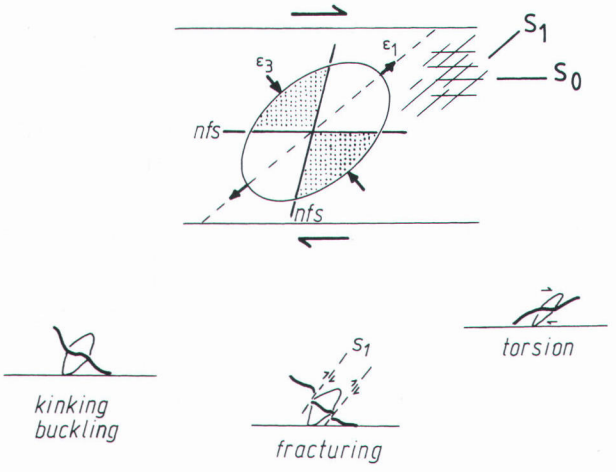

Figure 7. Possible orientation of *Ozarkodina* Pa elements in the "apparent flattening" framework, simplified to two dimensions (submeridional section parallel to stretching lineation) (S_0 = bedding; S_1 = cleavage). The "plane of no finite strain" (nfs) divides the finite strain ellipse in two compressional (dotted) and two extensional sectors (blank). While kinking, buckling, bending and fracturing can be explained by the flattening component, torsion needs a shear component.

6. Acknowledgements

The SEM-research was supported by a grant from the F.W.O. — Vlaanderen (Belgium), Project N° 2.0038.91. We acknowledge Dr. S. Schmid, Dr. T. Engelder and Dr. G. Oertel for their constructive comments on the original manuscript. Also Dr. D. Jongmans and Dr. E. Groessens are acknowledged for the final review. The paper is the reflection of an oral presentation ("Can Conodonts be used as strain markers?") at the Meuse-Rhine Euregion Meeting in Krefeld on 27.05.1994.

7. References

BEUGNIES, A., 1963. Le Massif cambrien de Rocroi. *Bulletin du Service de la Carte Géologique de France*, 270: 355-521.

BEUTNER, E.C. & CHARLES, E.G., 1985. Large volume loss during cleavage formation, Hamburg sequence, Pennsylvania. *Geology*, 13: 803-805.

BORREMANS, G. & BULTYNCK, P., 1986. Conodontes du calcaire de Naux — Gedinnien inférieur au sud immédiat du Massif de Rocroi (Ardenne française). *Aardkundige Mededelingen*, 3: 45-58.

BROADHEAD, T.W. & DRIESE, S.G., 1990. Gravitational settling of conodont elements: implications for paleoecological interpretations of conodont assemblages. *Geology*, 18: 850-853.

FLÜGEL, H. & ZIEGLER, W., 1957. Die Gliederung des Oberdevons und Unterkarbons am Steinberg westlich von Graz mit Conodonten. *Mitteilungen der naturwissenschaftliches Vereinigung Steiermark*, 87: 25-60.

HELSEN, S., 1994. Micromorphological changes in Pridolian/Lochkovian conodonts from the low-grade metamorphosed Naux Limestone (Ardennes, France). *Bulletin de la Société belge de Géologie*, 103: 205-217.

HELSEN, S. & KÖNIGSHOF, P., 1994. Conodont thermal alteration patterns in Palaeozoic rocks from Belgium, northern France and western Germany. *Geological Magazine*, 131: 369-386.

HUGON, H., 1983. Structures et déformation du Massif de Rocroi (Ardennes). *Bulletin de la Société Géologique et Minéralogique de Bretagne*, C15: 109-143.

KOVACS, S. & ARKAI, P., 1987. Conodont alteration in metamorphosed limestones from northern Hungary and its relationship to carbonate texture, illite crystallinity and vitrinite reflectance. *In* Austin, R.L., ed., Conodonts: Investigative Techniques and Applications, *British Micropalaeontological Society Series*. Ellis Horwood Ltd., Chichester, p. 209-300.

KÖNIGSHOF, P., 1992. Der Farbänderungsindex von Conodonten (CAI) in paläozoischen Gesteinen (Mitteldevon bis Unterkarbon) des Rheinischen Schiefergebirges — Eine Ergänzung zur Vitrinitreflexion. *Courier Forschungsinstitut Senckenberg*, 146: 1-118.

KOZUR, H. & MOCK, R., 1977. Conodonts and holothurian sclerites from the Upper Permian and Triassic of the Bükk Mountains (North Hungary). *Acta universitatis Szegediensis, Acta Mineralogica et petrographica*, 23: 109-126.

MASHKOVA, T.V., 1972. Ozarkodina steinhornensis (ZIEGLER) Apparatus, its Conodonts and Biozone. *Geologica et Palaeontologica*, SB1: 81-90.

MARCH, A., 1932. Mathematische Theorie der Regelung nach der Korngestalt bei affiner Deformation. *Zeitschrift fur Kristalografie*, 81: 285-297.

Mc GOFF, H.J., 1991. The hydrodynamics of conodont elements. *Lethaia*, 24: 235-247.

MEILLIEZ, F., 1984. La Formation de Fépin (Gedinnien de l'Ardenne): Un marqueur régional lithostratigraphique et structural. *Annales de la Société Géologique du Nord*, 103: 37-53.

MEILLIEZ, F., ANDRE L., BLIECK, A., FIELITZ, W., GOFETTE, O., HANCE, L., KHATIR, A., MANSY, J.-L., OVERLAU, P. & VERNIERS, J., 1991. Ardenne — Brabant. *Sciences géologiques, Bulletin*, 44: 3-29.

NORBY, R.D. & AVCIN, M.J., 1987. Contact microradiography of conodont assemblages. *In* Austin, R.L., ed., Conodonts: Investigative Techniques and Applications, *British Micropalaeontological Society Series*. Ellis Horwood Ltd., Chichester, p. 153-167.

RAMSAY, J.G. & HUBER, M.I., 1983. The technique of modern structural geology. Volume 1: Strain Analysis. Academic Press, 307 pp.

RAVEN, J.G.M. & VAN DER PLUIJM, B.A., 1986. Metamorphic fluids and transtension in the Cantabrian Mountains of northern Spain: an application of the conodont colour alteration index. *Geological Magazine*, 123: 673-681.

REJEBIAN, V.A., HARRIS, A.G. & HUEBER, J.S., 1987. Conodont color and textural alteration: An index to regional metamorphism,

contact metamorphism, and hydrothermal alteration. *Geological Society of America, Bulletin*, 99: 471-479.

SCHÖNLAUB, H.-P., FLAJS, G. & THALMANN, F., 1980. Conodontenstratigraphie am Steirischen Erzberg (Nördliche Grauwakkezone). *Jahrbuch der Geologisches Bundesamstalt Wien*, 123: 169-229.

SINTUBIN, M., 1994. Texture types in shales and slates. *In:* Bunge, H.L., Siegesmud, S., Skrotzki, W. & Weber, K., eds, Textures of Geological Materials. *DGM Informationsgesellschaft-Verlag*, 221-229.

ZIEGLER, W., 1960. Conodonten aus dem Rheinischen Unterdevon (Gedinnium) des Remscheider Sattels (Rheinisches Schiefergebirge). *Paläontologisches Zeitschrift*, 34: 169-201.

Manuscript received on 11.04.1995 and accepted for publication on 05.07.1997.

GEOLOGICA BELGICA (1998) 1: 49-53

Inductively coupled plasma-mass spectrometric (ICP-MS) analysis of silicate rocks and minerals

Jacqueline VANDER AUWERA, Guy BOLOGNE, Iwan ROELANDTS & Jean Clair DUCHESNE

(2 figures & 5 tables)

Laboratoires associés de Géologie, Pétrologie, Géochimie, Université de Liège, B-4000 Liège, Belgium.

ABSTRACT. The accurate measurement of low levels of trace elements is now necessary in most petrological studies. In this paper, we present the methods used in our laboratory ("Collectif interinstitutionnel de géochimie instrumentale") to analyse simultaneously, with the ICP-MS instrument, 26 trace elements in silicate rocks and minerals. Whole-rocks are prepared using a lithium metaborate fusion in order to assure dissolution of resistant mineral phases, whereas mineral separates (plagioclases, pyroxenes, apatites) are prepared using an open acid digestion. Calibration of the ICP-MS is made with international reference materials for whole-rocks and with synthetic aqueous solutions for mineral separates. The accuracy of the data as well as limits of quantification (LOQ) vary among elements but are usually very good (accuracy better than 6%, LOQ usually below 1 µg/g in solids). Combination of XRF and ICP-MS capabilities enables us to determine 38 elements (major and trace) on a routine basis.

KEYWORDS: Inductively coupled plasma mass spectrometry, trace elements geochemistry, sample preparation.

RESUME. Analyse des roches silicatées et des minéraux par spectrométrie de masse à plasma couplé inductivement. La mesure exacte de faibles quantités d'éléments en trace est maintenant nécessaire dans toute étude pétrologique. Dans ce papier, nous présentons les méthodes utilisées dans notre laboratoire («Collectif interinstitutionnel de géochimie instrumentale») pour analyser simultanément avec l'ICP-MS, 26 éléments en trace dans des roches silicatées et des minéraux séparés. Les échantillons de roches totales sont préparés à l'aide d'une fusion au métaborate de lithium, de manière à assurer la dissolution complète de phases minérales résistantes, alors que les minéraux séparés (plagioclases, pyroxènes, apatites) sont préparés à l'aide d'une attaque acide en bombes ouvertes. La calibration de l'ICP-MS se fait avec des standards internationaux dans le cas des roches totales et avec des solutions standards synthétiques pour les minéraux séparés. L'exactitude des données ainsi que les limites de quantification (LOQ) varient d'un élément à l'autre mais sont habituellement très bonnes (exactitude meilleure que 6 %, LOQ inférieure à 1 µg/g dans le solide). En combinant les capacités de la Fluorescence-X et de l'ICP-MS, nous avons maintenant la possibilité de déterminer en routine 38 éléments (majeurs et traces).

MOTS-CLES : Spectrométrie de masse à plasma couplé inductivement, géochimie des éléments en traces, préparation des échantillons.

1. Introduction

In most petrogenetic and geochemical studies, quantitative determination of a wide variety of elements is now required. In our laboratory, the "Collectif interinstitutionnel de géochimie instrumentale", major elements as well as selected trace elements (Ba, Ce, Co, Cr, Nb, Ni, Rb, Sr, V, Y, Zn, Zr) have been measured by XRF (Alpha 2020, CGR) for about twenty years (Bologne & Duchesne, 1991). Nevertheless, detection limits for this

technique are relatively high, usually between 10 to 25 µg/g. They thus preclude the determination of trace elements occurring at low contents in silicate rocks like REE, U, Th, Ta. In 1992, an ICP-MS VG Plasma Quad PQ2 from Fisons Instruments has thus been acquired to enlarge the analytical capacity of our laboratory. The aim of this paper is to present the analytical procedure followed here as well as some data on accuracy, precision and limits of quantification.

2. Sample preparation

Prior to being analysed by ICP-MS, rocks or mineral samples must be put into solution. Alkali fusion and open acid digestion are used in many geological laboratories and are well-established methods (Jarvis, 1992; Totland *et al.*, 1992). Nevertheless, the precise recipe varies between laboratories and the exact methods used at Liège are described here.

2.1. Alkali fusion

250 mg of powdered rock (sample or reference material) are weighed into a Pt crucible and mixed with 1.25 g of lithium metaborate (Aldrich, USA) (Jarvis, 1992; Totland *et al.*, 1992). The sample is fused over a Meker burner and an average of 15 min is usually required to completely fuse the sample. The hot melt is then poured directly into a beaker containing 150 ml of 0.8M HNO_3. Solution is mixed continuously on a magnetic stirrer until complete dissolution of all solids and finally diluted to 250 ml in a volumetric flask. Solutions are stored in polypropylene bottles and diluted to 1: 5000 prior to being analysed by ICP-MS. When total dissolved solids (TDS) in samples exceed 2000 µg/ml, they cause partial blocking of the sampling cone aperture and important signal drift with time. Dilution of 1: 5000 maintains the TDS below 2000 µg/ml.

2.2. Open acid digestion

Until now, in our laboratory, open acid digestion has been performed only on rocks deficient in trace elements and mineral separates (plagioclase, pyroxenes, apatite) as this method of sample preparation is time-consuming and does not assure complete dissolution of the sample when resistant accessory phases, usually rich in incompatible elements, are present. Minerals have been separated from whole rocks using classical separation techniques (Duchesne, 1966). 0.5 g of sample are weighed into clean Pt crucible and moistened with 2ml of distilled H_2O. 10 ml of HF and 2ml of HCl (pyroxenes) or HNO_3 (plagioclase) are added. The samples are allowed to stay in the acid mixture for several hours before the evaporation stage, as this improves the effectiveness of the acid digestion. The crucibles are then heated on a hot plate (170 °C) to incipient dryness. The acid digestion is repeated three times. 10 ml of HNO_3 are then added to the samples and the evaporation cycle is repeated three times in order to eliminate all traces of HF. When HCl has been used during the digestion (pyroxenes), 10 ml of H_2O are added to the samples after the acid digestion and samples are transferred into pyrex beakers in order to avoid mixing of HNO_3 and HCl in contact with Pt. The beakers are then put on the hotplate for evaporation: 10 ml of HNO_3 are added to the samples and the evaporation cycle is repeated three times in order to eliminate all traces of HCl. The samples are then transferred in 250 ml volumetric flasks and made to volume giving a dilution factor of 500. In the case of apatites, the digestion procedure is simplified as this mineral can be put into solution simply by adding 20% HNO_3. When the REE content is expected to be low in the sample (below 1 time chondrite levels), REE can be concentrated using the cation exchange technique (Roelandts & Michel, 1986).

Table 1. Instrumental operating conditions for trace element determination of the Liège ICP-MS (VG Plasma Quad PQ2).

Coolant gas-flow (Ar)	11.25 l/min
Auxiliary gas-flow (Ar)	0.65 l/min
Nebuliser gas-flow (Ar)	0.725 l/min
Nebuliser type	de Galan, high dissolved solids nebuliser
Forward power	1.35 kW
Reflected power	< 5 W
Washing time	150 s
Detector type	Galileo
Detector mode	Pulse counting
Acquisition mode	Peak jumping

3. Instrumentation

The ICP-MS instrument is a VG Elemental Plasma Quad PQ2. The operating conditions are given in Table 1. Samples are introduced with a peristaltic pump and a de Galan nebuliser is used. The "peak jumping mode" is preferred as this optimises counting times and the Galileo detector is set in the "pulse counting mode". In the case of whole-rock analyses, calibration is performed with five international reference materials (BE-N, DR-N, GS-N, GH, AC-E: these samples are currently being distributed by the CRPG, BP20, F54501 Vandoeuvre-lès-Nancy Cedex, France) and granite GA is used as a control. For mineral separates, standard solutions are prepared by diluting $1.000 gl^{-1}$ single element AAS standard solutions (Aldrich, USA) and the international reference material FK-N or one of our samples of known composition is used as a control. A blank solution prepared following the same procedure (alkali digest or open acid digestion) as the samples is also used in the calibration. For each sample or standard, data are acquired in 3 runs. $^{115}In + ^{187}Re + ^{209}Bi$ (50 ng/ml) are added to all samples and calibration solutions and are used as internal standards to correct for signal drift with time (see section 4). The isotopes chosen for the determination of each element are given in Table 2. Usually,

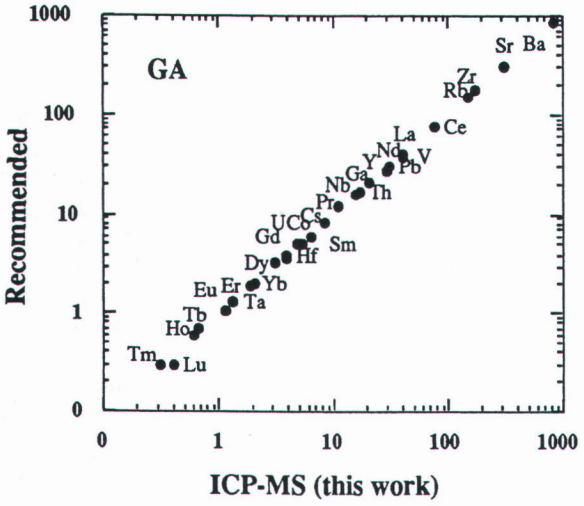

Figure 1. Comparison between recommended values (Govindaraju, 1995) and measured contents by ICP-MS for the international reference material GA.

the most abundant isotope, free of interferences and isobaric overlap, is selected. When several isotopes are determined for the same element, an average value is calculated.

4. Matrix, drift and interference problems

The sensitivity of one given element (counts per second per ng/g) is mainly controlled by its concentration but also by matrix effects like the presence of acids and the amount of TDS. As a perfect matrix match between standards and samples cannot be obtained, these interferences must be corrected with the use of internal standards. Moreover, as matrix effects also depend on the mass of the elements, three distinct internal standards (^{115}In, ^{187}Re, ^{209}Bi) are added to all solutions in order to cover the complete mass range. These spikes are also used to correct for the instrumental drift caused by progressive blocking of the cones apertures.

Interferences may arise from isobaric overlaps, the presence of doubly charged ions, and the formation of oxides and hydroxides (Table 2). The polyatomic forming reactions involve the plasma and atmospheric gases (O_2, N_2) as well as Cl, S which can be present in some solutions. The oxide level strongly depends on the plasma conditions. Significant molecular ion interferences occur below 80 amu (see for exemple Sc, V, Co, Cu, Ga in Table 2). Control of the oxide and hydroxide interferences has shown that in the case of geological materials, the severe interferences are the following: $^{135}Ba^{16}O$ and $^{134}Ba^{16}OH$ on ^{151}Eu; $^{137}Ba^{16}O$ and $^{136}Ba^{16}OH$ on ^{153}Eu; $^{141}Pr^{16}O$ on ^{157}Gd; $^{143}Nd^{16}O$ on ^{159}Tb; $^{150}Nd^{16}O$ on ^{166}Er. Correction factors for these interferences are monitored with synthetic standard solutions or calculated with interference equations introduced in the PQ vision software.

Table 2. Compilation of isotopes selected for analysis and quantification as well as potential spectral interferences.

Element	Abundance (%)	m/z	Interferences, remarks
Sc	100	45	$^{12}C^{16}O_2H$, $^{26}Mg^{16}OH$, $^{28}Si^{16}OH$, $^{29}Si^{16}O$, $^{44}CaH^+$, $^{38}Ar^7Li$ in fusion digests
V	99.76	51	$^{35}Cl^{16}O$, $^{34}S^{16}OH$, $^{36}Ar^{15}N$, $^{36}Ar^{14}NH$, $^{37}Cl^{14}N$, $^{36}S^{15}N$, $^{33}S^{18}O$
Co	100	59	$^{36}Ar^{23}Na$, $^{42}CaOH^+$, $^{43}Ca^{16}O$
Cu	69.2	63	$^{40}Ar^{23}Na$, $^{31}P^{16}O_2$, $^{47}Ti^{16}O$
	30.8	65	$^{49}Ti^{16}O$, $^{130}Ba^{++}$, $^{33}S^{16}O_2$, S_2
Zn	27.8	66	$^{50}Ti^{16}O$, $^{50}V^{16}O$, $^{50}Cr^{16}O$, $^{132}Ba^{++}$, SO_2, S_2
Ga	39.8	71	$^{36}Ar^{35}Cl$, $^{142}Ce^{2+}$, $^{142}Nd^{2+}$, $^{40}Ar^{31}P$, $^{35}Cl^{18}O_2$, SO_2, $^{38}Ar^{33}S$
Rb	72.2	85	$^{170}Er^{++}$, $^{170}Yb^{++}$
Sr	82.5	88	$^{40}Ar^{48}Ca$, $^{176}Lu^{++}$, $^{176}Yb^{++}$
Y	100	89	
Zr	51.5	90	
	11.2	91	
Nb	100	93	$^{56}Fe^{37}Cl$
In	95.7	115	Internal standard
Cs	100	133	
Ba	6.59	135	
	11.3	137	
La	99.9	139	
Ce	88.5	140	
Pr	100	141	
Nd	12.2	143	
	17.2	146	$^{130}Ba^{16}O$
Sm	15.1	147	$^{130}Ba^{16}OH$
	14	149	$^{132}Ba^{16}OH$
Eu	47.8	151	$^{135}Ba^{16}O$. $^{134}Ba^{16}OH$
	52.2	153	$^{137}Ba^{16}O$. $^{136}Ba^{16}OH$
Gd	15.7	157	$^{141}Pr^{16}O$. $^{140}Ce^{16}OH$
Tb	100	159	$^{143}Nd^{16}O$
Dy	18.9	161	$^{145}Nd^{16}O$
	25	163	$^{147}Sm^{16}O$
Ho	100	165	$^{149}Sm^{16}O$
Er	33.4	166	$^{150}Nd^{16}O$. $^{150}Sm^{16}O$
	22.9	167	$^{151}Eu^{16}O$
Tm	100	169	$^{153}Eu^{16}O$
Yb	21.8	172	$^{156}Gd^{16}O$. $^{156}Dy^{16}O$
	16.1	173	$^{157}Gd^{16}O$
Lu	97.4	175	$^{159}Tb^{16}O$
Hf	18.5	177	$^{161}Dy^{16}O$
	27.1	178	$^{162}Dy^{16}O$. $^{162}Er^{16}O$
Ta	99.9	181	$^{165}Ho^{16}O$
Re	62.9	187	Internal standard
Pb	23.6	206	
	22.6	207	
	52.3	208	
Bi	100	209	Internal standard
Th	100	232	
U	99.3	238	

Memory effects can occur during ICP-MS analysis and correspond to an enhancement of the signal produced by erosion of elements deposited along the sample path during the analysis of previous samples. We observed significant memory effects for Cu as well as for Zr, Hf, Nb and Ta. These problems are reduced by using a washout solution containing 5% HNO_3 and long washing times (150s).

5. Detection and quantification limits, accuracy, precision

It has been shown that ICP-MS has higher sensitivity and lower instrumental detection limits than other rapid multi-element techniques. Following the recommendations of Jarvis (1992), we have distinguished detection limits and lower limits of quantitative analysis. Instrumental detection limits, usually given as 3s on 11 determinations of the signal produced by a blank solution, give estimates of the technical performance of a specific instrument but do not correspond to realistic detection limits for quantitative analysis, as the errors at the level of detection limits are very high. Consequently, the limits of quantitative determination (LOQ) are based on 11 determinations of the signal produced by a "blank reagent" solution (containing $LiBO_2$, HNO_3, H_2O) and the lower limits of quantification are determined by using ten sigma standard deviation as proposed by the "American Society Committee on Environmental Improvement" (Jarvis, 1992). These limits of quantitative determinations, based on 12 separate runs, are reported in Table 3 (LOQ) and are expressed as concentrations (µg/g) in the solid. These LOQ are similar to those proposed in the literature (Jarvis, 1990).

The accuracy of the method is controlled by comparing our ICP-MS results obtained on the reference material GA with the recommended values of Govindaraju (1995). Results shown in% in Table 3 and Fig. 1 indicate that the accuracy is usually very good except for Lu (34.3%), whose content in GA is close to the LOQ. Analyses of mineral separates (plagioclase, apatite, orthopyroxene) are shown on Fig. 2. In Table 4, the REE content, measured in the international reference material FK-N are presented. FK-N was prepared with an open acid digestion and REE were preconcentrated with the ion-exchange technique (Roelandts & Michel, 1986).

In order to determine the long term precision of the method, the reference materials GA, GS-N, DR-N and BE-N have been included in several runs (15). As indicated in Tables 3 & 5, the accuracy and precision obtained on these four distinct compositions are usually very good, especially for the REE. In the case of Sr, Ba and Zr, the precision is not as good as for the other elements. This probably results from a higher background for Sr and Ba and memory effects for Zr.

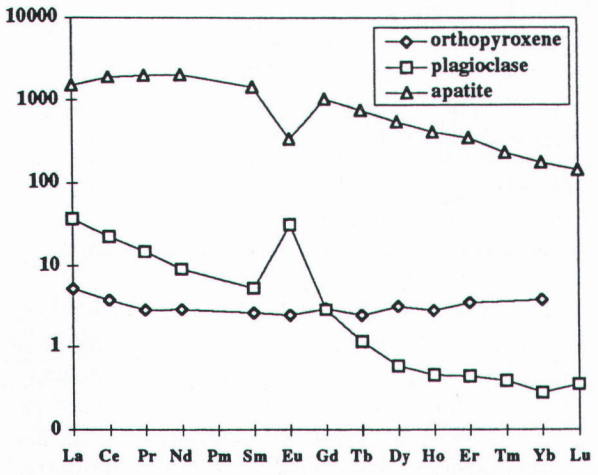

Figure 2. REE patterns normalized to chondrites (Sun & Mc Donough, 1989) of plagioclase, apatite and orthopyroxene.

Table 3. Accuracy, precision and limits of quantification.

	GA/ICP-MS µg/g n=11 independent analyses (this work)	GA/REC (1) µg/g	+/– CL (2) µg/g	Acc %	LOQ µg/g in solids
Rb	174±3	175	5	0.8	0.32
Sr	308±21	310	12	0.6	1.22
Y	20.2±2.4	21.0	2.0	4.0	0.57
Zr	150±13	150	12	0.2	5.00
Nb	10.7±1.9	12.0	1.6	10.8	1.31
Cs	6.46±0.10	6.00	0.50	7.6	0.15
Ba	846±17	840	22	0.7	3.95
La	40.7±1.2	40.0	3.0	1.7	0.50
Ce	77.4±2.6	76.0	4.0	1.8	0.10
Pr	8.5±0.3	8.30	0.30	2.0	0.07
Nd	28.9±1.3	27.0	3.0	7.1	0.62
Sm	5.37±0.20	5.00	0.50	7.4	0.47
Eu	1.14±0.0	1.08	0.05	5.8	0.09
Gd	3.90±1.0	3.80	0.30	2.7	0.77
Tb	0.62±0.1	0.60	0.10	2.7	0.12
Dy	3.13±0.3	3.30	0.30	5.2	0.18
Ho	0.66±0.1	0.70	0.10	5.7	0.06
Er	1.89±0.1	1.90	0.20	0.7	0.12
Tm	0.31±0.0	0.30	0.04	2.3	0.03
Yb	2.06±0.1	2.00	0.20	3.0	0.12
Lu	0.40±0.2	0.30	0.03	34.3	0.04
Hf	3.82±0.8	4.00	0.30	4.5	0.80
Ta	1.32±0.2	1.30	0.20	1.6	0.15
Pb	31.1±1.7	30.0	3.0	3.6	1.24
Th	17.5±0.8	17.0	1.8	3.2	0.10
U	5.19±0.4	5.00	0.50	3.9	0.22

1. Recommended values from Govindaraju (1995).
2. 95% confidence limits (CL) from Govindaraju (1995).

Table 4. Results obtained for standard FK-N.

	FK-N This work	FK-N (1) Recommended values
La	1.008	1 (0.95 (2))
Ce	1.17	1
Pr	0.099	0.09 (2)
Nd	0.353	0.3
Sm	0.058	0.06 (0.05 (2))
Eu	0.405	0.42 (0.45 (2))
Gd	0.069	0.05 (0.06 (2))
Tb	<0.05	0.01
Dy	0.065	0.06
Ho	<0.05	0.012 (2)
Er	<0.05	0.04
Tm	<0.05	0.006 (2)
Yb	0.052	0.04
Lu	<0.05	0.01 (0.006 (2))

1. Govindaraju & Roelandts (1989).
2. Govindaraju (1995).

Table 5. Results obtained on three international reference materials.

	GS-N		DR-N		BE-N	
	X (1)	REC(2)	X (1)	REC(2)	X (1)	REC(2)
Rb	186±4	185	74±2	73	49±2	47
Sr	576±22	570	397±16	400	1401±72	1370
Y	16.0±1.1	16.0	26±1	26	29±1	30
Zr	218±13	235	132±9	125	262±11	260
Nb	21.9±1.3	21.0	7.2±1.0	7.0	110±7	105
Cs	5.5±0.2	5.4	6.2±0.2	6.3	0.7±0.1	0.8
Ba	1393±22	1400	382±9	385	1037±37	1025
La	71.0±3.1	75.0	21.5±1.0	21.5	82±1	82
Ce	133.5±4.3	135.0	44.8±1.6	46.0	153±3	152
Pr	14.5±0.6	14.5	5.7±0.2	5.7	17.6±0.4	17.5
Nd	48.5±2.2	49.0	23.2±0.6	23.5	67±1	67
Sm	7.3±0.3	7.5	5.2±0.2	5.4	12.1±0.4	12.2
Eu	1.6±0.1	1.7	1.47±0.03	1.45	3.7±0.2	3.6
Gd	4.9±0.3	5.2	4.9±0.2	4.7	9.9±0.5	9.7
Tb	0.60±0.02	0.60	0.8±0.0	0.77	1.28±0.04	1.30
Dy	3.0±0.1	3.1	4.5±0.2	4.6	6.3±0.2	6.4
Ho	0.57±0.03	0.60	0.98±0.04	1.00	1.1±0.1	1.1
Er	1.4±0.1	1.5	2.6±0.1	2.5	2.4±0.1	2.5
Tm	0.22±0.01	0.22	0.38±0.02	0.39	0.33±0.02	0.34
Yb	1.4±0.1	1.4	2.5±0.1	2.5	1.8±0.1	1.8
Lu	0.21±0.03	0.22	0.38±0.02	0.40	0.25±0.03	0.24
Hf	6.2±0.2	6.2	3.4±0.2	3.5	5.8±0.1	5.6
Ta	2.4±0.1	2.6	0.6±0.1	0.6	4.9±1.0	5.7
Pb	56.3±1.2	53.0	54.7±0.9	55.0	4.3±0.4	4
Th	42.1±1.6	41.0	4.7±0.4	5.0	10.9±0.4	10.4
U	7.7±0.4	7.5	1.5±0.1	1.5	2.4±0.2	2.4

1. Average of 15 independent analyses.
2. Govindaraju (1995).

6. Conclusions

A routine method has been developped for simultaneous determination of 26 trace elements by ICP-MS. Application of the method has shown that accuracy is good or excellent for 24 elements. The limits of quantification are much lower (0.03 to 5 µg/g) than those obtained for XRF. A clear advantage of the ICP-MS is that a multi-element data set can be obtained with one single instrument, and ICP-MS also appears as a very good technique for the determination of REE. Moreover, combination of XRF and ICP-MS capabilities enables us to determine 38 elements on a routine basis.

7. Acknowledgements

Acquisition and installation of the ICP-MS was made possible by a FRFC convention (2.4508.91) together with a Lotto grant (9.4808.90).

8. References

BOLOGNE, G. & DUCHESNE, J. -C., 1991. Analyse des roches silicatées par spectrométrie de fluorescence X: précision et exactitude. *Service Géologique de Belgique, Professional Paper,* 249.

DUCHESNE, J.-C., 1966. Séparation rapide des minéraux des roches. *Annales de la Société Géologique de Belgique,* 89: 347-356.

GOVINDARAJU, K. & ROELANDTS, I., 1989. 1988 compilation report on trace elements in six ANRT rock reference samples: diorite DR-N, serpentine UB-N, bauxite BX-N, disthene DT-N, granite GS-N and potash feldspar FK-N. *Geostandards Newsletter,* 13: 5-67.

GOVINDARAJU, K., 1995. 1995 working values with confidence limits for twenty-six CRPG, ANRT and IWG-GIT geostandards. *Geostandards Newsletter,* 19, Special Issue July: 1-32.

JARVIS, I., 1992. Sample preparation for ICP-MS. In Jarvis, K., Gray, A. & Houk, R., eds, Handbook of inductively coupled plasma mass spectrometry. Blackie, Glasgow, p. 172-224.

JARVIS, K., 1990. A critical evaluation of two sample preparation techniques for low-level determination of some geologically incompatible elements by inductively coupled plasma-mass spectrometry. *Chemical Geology,* 83: 89-103.

ROELANDTS, I. & MICHEL, G., 1986. Sequential inductively coupled plasma determination of some rare-earth elements in five French geostandards. *Geostandards Newsletter,* 10: 135-154.

SUN, S.S. & McDONOUGH, W.F., 1989. Chemical and isotopic systematics of oceanic basalts: implications for mantle composition and processes. In Saunders, A. D., & Norry, M. J., eds, Magmatism in the ocean basins. Geological Society Special publication n° 42, Blackwell Scientific Publications, p. 313-345.

TOTLAND, M., JARVIS, I. & JARVIS, K., 1992. An assessment of dissolution techniques for the analysis of geological samples by plasma spectrometry. *Chemical Geology,* 95: 35-62.

Manuscript received on 05.03.1996 and accepted for publication on 02.02.1997.